PET data: processing, statistical analyses and partial volume effect (PVE) correction

PET data evaluation, normalization, voxel-based analyses & group comparisons

^{18}F-FDG- and ^{11}C-PiB-PET recordings were performed with the same Siemens ECAT HR+ scanner (CTI, Knoxville, Tennessee, USA) in 3D mode, while structural T1w MRI examinations were performed on a Siemens 1.5 Tesla Magnetom Symphony scanner (Siemens AG, Erlangen, Germany).

The first step of the PET data evaluation consisted of a visual consideration of all individual reconstructed ^{11}C-PiB- and ^{18}F-FDG-PET images and basic image processing, such as normalization followed by statistical group analyses using statistical parametric mapping software 5 (SPM5, Wellcome Department of Cognitive Neurology, London, UK) in MATLAB 7.5.

The structural T1w MRI datasets were spatially normalized to the SPM standard MRI T1 template in the Montreal Neurological Institute (MNI) space using default transformation parameters. Afterwards, BL as well as FU ^{11}C-PiB and ^{18}F-FDG images were co-registered to each individual BL or FU volumetric MRI and spatially normalized to the T1 MRI MNI template using warping parameters derived from the individual MRI normalization (*1-4*). Normalized images were represented on a 79x95x69 matrix with 2x2x2 mm voxel-size and smoothed, like previously published (*2, 5*), with an isotropic Gaussian full-width-at-half-maximal kernel of 12mm.

Voxel-wise whole brain group comparisons (AD-patients (FU & BL) vs. HC1) were calculated in the neurobiologically expected directions with a consistent probability threshold of $p<0.01$, false discovery rate (FDR) corrected for multiple comparisons, and a threshold for minimum spatial extent of 20 contiguous voxels throughout all PET analyses.

Partial volume effect (PVE) correction

To correct ^{18}F-FDG-PET as well as ^{11}C-PiB-PET data for a potential influence of regional cortical atrophy, a correction for partial volume effects (PVE) was performed in AD patients' (BL & FU scans) as well as in control subjects' scans with an algorithm implemented in the PMOD software package (PMOD Technologies Ltd., Adliswil, Switzerland) (*1*). After coregistration of individual PET and MRI data, a segmentation of each T1w MRI in grey matter (GM), white matter (WM) and cerebrospinal fluid (CSF) was carried out. The segmented MR data were then used for PVE correction of the PET data of every subject. Afterwards, the PVE-corrected PET data were normalized as described above.

1. Drzezga A, Grimmer T, Henriksen G, et al. Imaging of amyloid plaques and cerebral glucose metabolism in semantic dementia and Alzheimer's disease. *Neuroimage.* 2008;39:619-633.

2. Forster S, Yousefi BH, Wester HJ, et al. Quantitative longitudinal interrelationships between brain metabolism and amyloid deposition during a 2-year follow-up in patients with early Alzheimer's disease. *Eur J Nucl Med Mol Imaging.* 2012;39:1927-1936.

3. Grimmer T, Henriksen G, Wester HJ, et al. Clinical severity of Alzheimer's disease is associated with PIB uptake in PET. *Neurobiol Aging.* 2009;30:1902-1909.

4. Ziolko SK, Weissfeld LA, Klunk WE, et al. Evaluation of voxel-based methods for the statistical analysis of PIB PET amyloid imaging studies in Alzheimer's disease. *Neuroimage.* 2006;33:94-102.

5. Forster S, Grimmer T, Miederer I, et al. Regional expansion of hypometabolism in Alzheimer's disease follows amyloid deposition with temporal delay. *Biol Psychiatry.* 2012;71:792-797.

Assessment of annual amyloid changes

The two co-registered and spatially normalized ^{11}C-PiB-PET images (BL & FU) were quantitatively normalized (scaled) using the cerebellar vermis as reference region. In a second step, these images were smoothed using a Gaussian full-width at half-maximum filter of 6.5x6.5x5mm. Afterwards, ^{11}C-PiB annual rate of change (ARC-) images were created for each individual subject using the SPM Image Calculator and the following formula:

FU-^{11}C-PiB-scan minus BL-^{11}C-PiB-scan divided by follow-up duration in years

These ^{11}C-PiB ARC-images were smoothed a second time using a Gaussian filter of 10.3x10.3x10.3mm full-width at half-maximum.

Resting-state fMRI: Data acquisition parameters and pre-processing steps

For analysis of intrinsic functional connectivity in an independent group of healthy elderly control subjects (HC2), MRI was performed on a 3T whole body MR scanner (Achieva, Philips, Netherland) using an 8-channel phased-array head coil. All participants underwent 5 min of structural MRI and 10 min of resting-state fMRI. For co-registration and volumetric analysis, T1-weighted anatomical data were obtained from each subject by using a magnetization-prepared rapid acquisition gradient echo sequence (echo time [TE] = 4msec, repetition time [TR] = 9msec, inversion time [TI] = 100msec, flip angle = 5°, field of view [FoV] = 240 x 240 mm², matrix = 240 x 240, 170 slices, voxel size = 1 x 1 x 1 mm). fMRI data were collected using a gradient echo EPI sequence (TE = 35ms, TR = 2000ms, flip angle = 82°, FoV = 220 x 220 mm², matrix = 80 x 80, 32 slices, slice thickness = 4 mm, and 0 mm interslice gap); 10 minutes of scanning result in 300 volumes for the resting state.

SPM5 was used for motion correction, spatial normalization into the stereotactic MNI space and spatial smoothing with an 8 x 8 x 8 mm Gaussian kernel. The first three functional scans of each fMRI-session were discarded due to magnetization effects for each participant.

The time courses of the BOLD signals of all voxels within the ROI were extracted, Butterworth bandpass-filtered for frequencies ranging from 0.009 to 0.08 Hz and reduced to a ROI-representative time course by singular value decomposition. For ROI-based functional connectivity analysis, this time-course was put into a first-level fixed-effects general linear model and a voxel-wise multiple regression was performed to calculate a correlation map for each subject between the BOLD time-course extracted from the ROI and the time courses from all other voxels within the brain. Regressors for global grey matter (GM), white matter (WM) and cerebrospinal fluid (CSF) signal for each subject were included as covariates of no interest in each model (*1*, *2*).

To identify brain regions showing a significant positive intrinsic functional connectivity with the seed, group analyses were performed across this healthy elderly population using the same thresholds as for PET-data analyses ($p < 0.01$, FDR-corrected).

1. Fox MD, Snyder AZ, Vincent JL, Corbetta M, Van Essen DC, Raichle ME. The human brain is intrinsically organized into dynamic, anticorrelated functional networks. *Proc Natl Acad Sci U S A.* 2005;102:9673-9678.

2. Hedden T, Van Dijk KR, Becker JA, et al. Disruption of functional connectivity in clinically normal older adults harboring amyloid burden. *J Neurosci.* 2009;29:12686-12694.

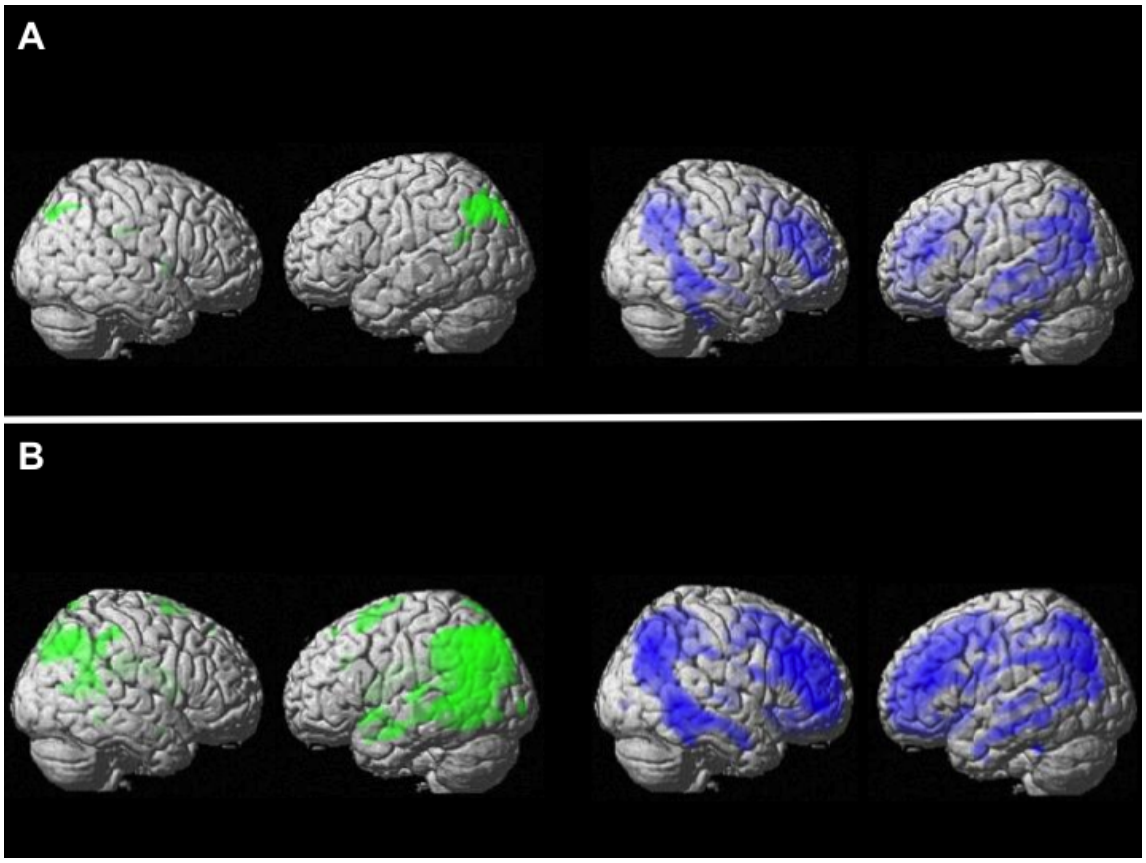

Supplemental Figure 1: A: Hypometabolism (green; revealed by Fluorodeoxyglucose (^{18}F-FDG PET)) and amyloid-deposition (blue; revealed by Pittsburg Compund B (^{11}C-PiB PET)) in 15 AD-patients compared with 15 elderly healthy control subjects at baseline point of time; $p<0.01$, false discovery rate (FDR-corrected). Partial volume effect (PVE)-corrected data. Results are displayed on a standard MRI-template.

B: Hypometabolism (green; revealed by ^{18}F-FDG PET) and amyloid-deposition (blue; revealed by ^{11}C-PiB PET) in 15 AD-patients compared with 15 elderly healthy control subjects at follow-up point of time; $p<0.01$, false discovery rate (FDR-corrected). Partial volume effect (PVE)-corrected data. Results are displayed on a standard MRI-template.

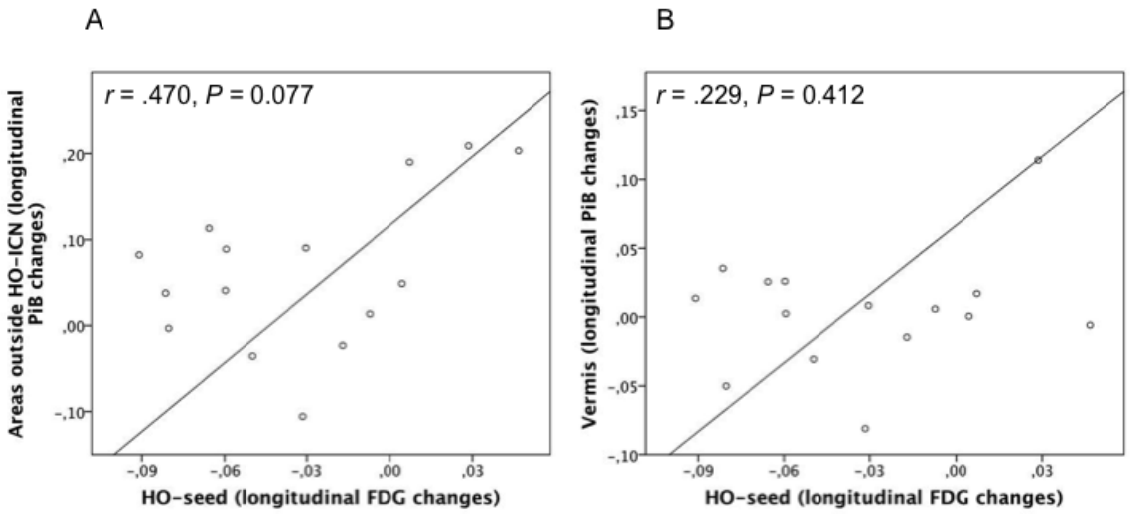

Supplemental Figure 2: Correlations between longitudinal changes of metabolism in the hypometabolism-only (HO)-seed and longitudinal changes of amyloid-uptake in non-connected brain-areas (areas outside the HO-ICN (intrinsic connectivity network; A)) resp. between longitudinal changes of metabolism in the HO-seed and longitudinal changes of amyloid-uptake in the cerebellar vermis (B).

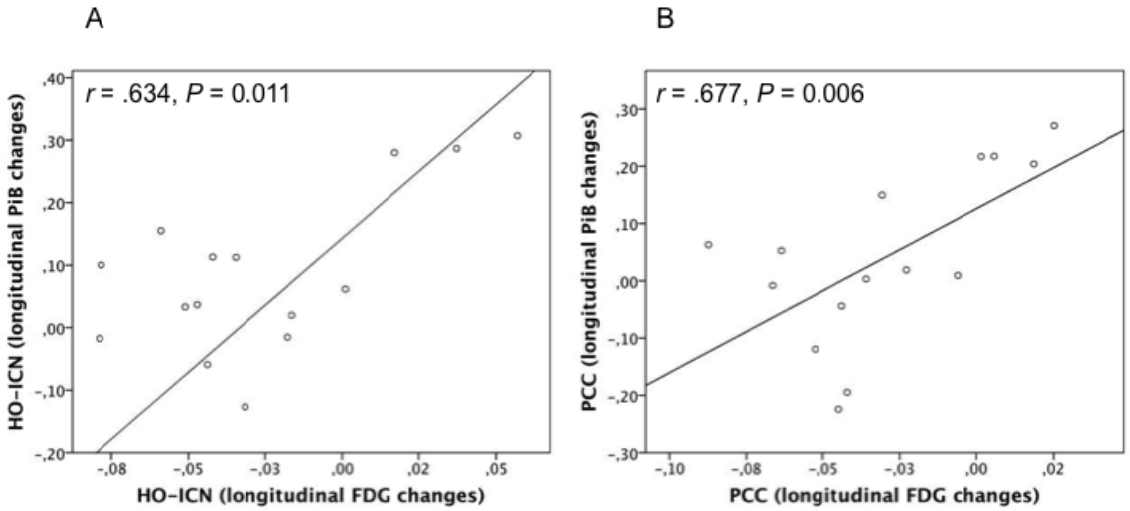

Supplemental Figure 3: Correlations between longitudinal changes of metabolism and longitudinal changes of amyloid-uptake loco-regional within the hypometabolism only-intrinsic connectivity network (HO-ICN; A) resp. within the posterior cingulate cortex (PCC; B).